Resistance Assessment of Microbial Electrosynthesis for Biochemical Production to Changes in Delivery Methods and CO_2 Flow Rates

Bin Bian[1], Jiajie Xu[1], Krishna P. Katuri[1], Pascal E. Saikaly[1*]

[1]*Biological and Environmental Sciences and Engineering (BESE) Division, Water Desalination and Reuse Center (WDRC), King Abdullah University of Science and Technology, Thuwal 23955-6900, Kingdom of Saudi Arabia*

[*] Corresponding author: Pascal E. Saikaly, PhD, email: pascal.saikaly@kaust.edu.sa

Abstract

Microbial electrosynthesis (MES) for CO_2 valorization could be influenced by fluctuations in CO_2 mass transfer and flow rates. In this study, we developed an efficient method for CO_2 delivery to cathodic biofilm by directly sparging CO_2 through the pores of ceramic hollow fiber wrapped with Ni-foam/carbon nanotube electrode, and obtained 45% and 77% higher acetate and methane production, respectively. This was followed by the MES stability test in response to fluctuations in CO_2 flow rates varying from 0.3 ml/min to 10 ml/min. The biochemical production exhibited an increasing trend with CO_2 flow rates, achieving higher acetate (47.0 ± 18.4 mmol/m^2/day) and methane (240.0 ± 32.2 mmol/m^2/day) generation at 10 ml/min with over 90% coulombic efficiency. The biofilm and suspended biomass, however, showed high resistance to CO_2 flow fluctuations with *Methanobacterium* and *Acetobacterium* accounting for 80% of the total microbial community, which suggests the robustness of MES for onsite carbon conversion.

Keywords: Microbial electrosynthesis, CO_2 flow fluctuation, Biochemical production, CO_2 valorization, Carbon capture and utilization

1. Introduction

Microbial electrosynthesis (MES) has emerged in recent years as a promising platform for sustainable CO_2 reduction, green chemical production and renewable energy storage in circular carbon bioeconomy (Jung et al., 2020). In MES system, chemolithoautotrophs growing on the MES cathode surface efficiently utilize the reducing equivalents (i.e., electrons or H_2), which could be provided by renewable energy sources, for CO_2 reduction and biochemical generation (Rojas et al., 2018). As microbial catalysts are much cheaper and more sustainable (i.e., self-regenerating) compared to precious metal-based inorganic catalysts for electrochemical CO_2 reduction, MES is regarded as an environment-friendly technology with the potential for on-site CO_2 capture and utilization to mitigate global warming (Rojas et al., 2018).

Most studies on MES have mainly focused on the development of cathode materials (Bajracharya et al., 2016; Jourdin et al., 2015), selection of highly-efficient microbes (Aryal et al., 2017b), and generation of diverse biochemicals such as butyrate (Bajracharya et al., 2016) and caproate (Jourdin et al., 2019) from CO_2. The high market value and stable chemical formula of these biochemicals make MES from CO_2 using renewable electricity highly attractive (Jourdin et al., 2019). To enhance the rates of CO_2 reduction and biochemical production in MES, and hence the economic viability of MES, three-dimensional electrodes, such as reticulated vitreous carbon (RVC) deposited with multiwalled carbon nanotubes (MWCNT) (Jourdin et al., 2016a; Jourdin et al., 2015) or graphene (Aryal et al., 2017a), have been utilized as MES cathode with improved surface area and biocompatibility. Gas diffusion electrode (Bajracharya et al., 2016) and porous hollow fiber membrane cathodes (Alqahtani et al., 2018) have been recently developed for

enhancing microbial growth and delivering CO_2 gas directly to microbes, in order to buffer the cathodic surface pH (Lu et al., 2020) during CO_2 reduction, minimize the additional cost for using CO_2 sorbents, and mimic its real-field application for CO_2 flue gas capture (Katuri et al., 2018). A 56% higher acetate production was obtained with direct CO_2 delivery through Ni-based hollow fiber membrane cathode, which is believed to enhance the CO_2 mass transfer in MES compared to CO_2 sparging into the media (Bian et al., 2018). However, studies on the effect of continuous CO_2 flow (either directly through MES biocathode or indirectly through medium sparging) on MES performance and microbial community are lacking.

Besides, the CO_2 flow rate from an industrial source (anaerobic digestion, natural gas processing, etc.) will typically vary over time (Anantharaman et al., 2013). For example, the flow rates of CO_2 stream from power plants could fluctuate significantly within one day as a function of utility demand, while the production of biogas containing a large portion of CO_2 from anaerobic digesters usually varies on a seasonal basis due to temperature fluctuations (Peces et al., 2013). These fluctuations in CO_2 flow rates could alter the pH and CO_2 availability at the microbe-cathode interface, and might adversely affect the stability of microbial community and thus biochemical generation in MES. Therefore, examining the resistance of MES system to fluctuations in CO_2 flow rates is an important step before implementing MES system for onsite CO_2 capture and utilization from various industries.

It has been reported that microbial communities in MES were resilient to fluctuations or interruptions in electric supply (Rojas et al., 2018). In a recent study, adjustments in CO_2 loading rate and hydraulic retention time resulted in enhanced butyrate and caproate production through bioelectrochemical chain elongation (Jourdin et al., 2019). However, no

data has been presented whether the microbial community in MES cathode chamber were resistant or adapted to changes in CO_2 loading rate. To the best of our knowledge, studies on the effect of fluctuations in CO_2 flow rates on MES performance and microbial community structure are lacking. Therefore, the objective of this study was to examine the resistance of MES in terms of performance and microbial community structure to different delivery methods of CO_2 and to fluctuations in CO_2 flow rates. To achieve this objective, MES was first operated with two different delivery methods of CO_2 at a constant flow rate, either directly through ceramic hollow tube wrapped with electrically conductive biocathode or indirectly by sparging CO_2 into the medium through electrically insulated ceramic hollow tube, to determine their effect on MES performance and microbial community. Subsequently, the effects of four different CO_2 flow rates (0.3, 1, 3 and 10 ml/min) on current density, biochemical production from CO_2, and microbial community (biofilm and suspension) were evaluated in MES reactors operated at a fixed cathode potential (–0.8V vs. Ag/AgCl).

2. Experimental

2.1. Preparation of cathode and MES reactor construction

Two-chamber MES reactors were constructed using two glass bottles (300 ml each) separated by a Nafion ion exchange membrane (VWR, UK) (Scheme 1). Titanium plate (18 cm^2, Kunshan Tengerhui) was chosen as MES anode, and nickel foam (35 cm^2, Kunshan Tengerhui) coated with multi-walled carbon nanotubes (MWCNTs, Shenzhen Nanotech) served as MES cathode. The MWCNTs were electrophoretically deposited onto the Ni foam following the same procedure as in Bian et al (Bian et al., 2018). After MWCNT deposition, the Ni foam/CNT was tightly wrapped with a sewing nickel wire around a

ceramic hollow tube (CHT, outer diameter: ~1.2 cm, length: 9 cm, average pore size: ~ 1 μm) and was denoted as CHT/Ni foam/CNT cathode for abiotic and biotic experiment later. This approach for making hollow tube membrane cathodes is much simpler compared to the fabrication of metal-based hollow fiber membrane cathodes in previous studies (Alqahtani et al., 2018; Bian et al., 2018). The CHT/Ni foam/CNT could serve as a cathode and a gas delivery membrane for direct delivery of CO_2 through the pores of the ceramic membrane.

To examine the variation of MES performances induced by the two different delivery methods, two CHTs (a bare CHT and a CHT wrapped with the Ni foam/CNT cathode) were used. The bottom ends of both CHTs were sealed with epoxy, while the other ends were connected to a gas-tight Tygon pump tubing (Masterflex) for direct or indirect CO_2 delivery (Scheme 1). A 10-L gasbag with an inlet and outlet was connected to the other end of the Tygon tubing and the cathode chamber headspace, respectively, for gas recirculation. The junction of the Tygon tubing and CHT was covered with epoxy glue to make the CHT gas-tight before submersion into 275 ml DSMZ 879 media with 2.5 mM of sodium 2-bromoethanesulfonate (Na-2-BES) addition to inhibit methanogenesis. The medium had the following composition (L^{-1}): 1.0 g NH_4Cl, 0.1 g KCl, 0.2 g $MgSO_4 \cdot 7H_2O$, 0.8 g NaCl, 0.1 g KH_2PO_4, 0.02 g $CaCl_2 \cdot 2H_2O$, 10 ml trace element solution and 10 ml vitamin solution (DSMZ medium 141). $NaHCO_3$ (1g/L) was added to maintain a relatively stable HCO_3^- /CO_3^{2-} concentration in MES. Yeast extract, Na-resazurin, D-Fructose, L-Cysteine and Na_2S were omitted during the whole experimental period, while $MgSO_4 \cdot 7H_2O$ was replaced with $MgCl_2$ (0.08 g/L) after the enrichment stage to avoid possible sulfate

reduction in the cathode chamber. The same media without Na-2-BES was used as MES anolyte.

2.2. MES reactor operation

Replicate MES reactors were operated in batch mode at 30°C and at a fixed cathode potential of –0.8 V vs. Ag/AgCl reference electrode (3M KCl) (VMP3, Bio-Logic Science Instruments). The long-term biotic operation of MES was divided into three phases: Phase I (~ 150 days) to enrich chemolithoautotrophs on the MES cathode; Phase II (50 days) to test the effect of different CO_2 delivery methods; and Phase III (100 days) to test the effect of different CO_2 flow rates on MES performance and microbial community. A summary of the operation conditions during different phases is shown in Table 1. Abiotic study was conducted in the first batch of MES operation.

In Phase I, 10 ml of anaerobic sludge, obtained from an anaerobic digester for biogas production (Bian et al., 2020b), was added as an inoculum to enrich chemolithoautotrophs on CHT/Ni foam/CNT cathode surface. Bicarbonate was used as the sole carbon source and no CO_2 gas was sparged during this phase. The MES reactors were operated for 15-25 days per batch to avoid inoculum washout. The enrichment process took around 150 days to achieve stable biochemical production. Samples for microbial community analysis were taken from the biocathode at the end of Phase I.

In Phase II, the effect of indirect vs. direct delivery of CO_2 to the biofilm on CHT/Ni foam/CNT cathode at a fixed flow rate of 1 ml/min was examined after the completion of Phase I. To buffer the surface pH and minimize CO_2 mass transfer limitation to the biofilm on the cathode surface, pure CO_2 gas from the 10-L gasbag was directly delivered, using a peristaltic pump (Masterflex L/S, Cole-Parmer Instrument Ltd), through the pores in the

CHT/Ni foam/CNT cathode following a similar pumping strategy by Ojeda et al. (Ojeda et al., 2017). The effluent gas from the cathode chamber headspace was re-pumped into the gasbag for gas recirculation and analysis. For indirect CO_2 delivery, pure CO_2 from the 10-L gasbag was sparged through the pores of the plain CHT, which was placed at a distance of 2 cm from the CHT/Ni foam/CNT biocathode, following the same pumping and recirculation strategy as above, and CO_2 was transferred to the biofilm on the CHT/Ni foam/CNT cathode via diffusion in the catholyte (Scheme 1). Each condition (i.e., direct vs. indirect CO_2 delivery) was maintained for two batches (~ 25 days). Linear sweep voltammetry (LSV) from open circuit voltage of the system to –1 V vs. Ag/AgCl at a scan rate of 5 mV/s was conducted for the different delivery methods at the same pH with MES biocathode as working electrode, while Ti anode served as the counter electrode and Ag/AgCl as the reference electrode. Samples of biofilm on MES cathode and suspension were collected for amplicon sequencing at the end of the second batch for both direct and indirect CO_2 delivery.

In phase III, four different CO_2 flow rates were selected to determine their effect on MES performance and microbial community. The rates of CO_2 sparged through the pores of CHT/Ni foam/CNT biocathode were varied stepwise from low to high (0.3, 1.0, 3.0 and 10.0 ml/min) every two batches (~25 days). LSV was conducted following the same procedure as above. Samples of biofilm on MES cathode and suspension were collected for amplicon sequencing at the end of the second batch for each flow rate.

2.3. Flow cytometry

Suspended cells were quantified using flow cytometry (FCM, Accuri C6, BD Biosciences) at the end of the second batch for the different CO_2 delivery methods and flow rates.

Briefly, 1 ml sample was taken from the cathode chambers and diluted 10000× before being stained with SYBR Green. The FCM, equipped with volumetric counting hardware, measured the particle number in 50 μl sample medium at a pre-set flow rate of 35 μl/min, with Milli-Q water in between for cleaning (Prest et al., 2014).

2.4. Chemical analysis and efficiency calculation

Liquid and gas samples were collected and analyzed every 3-5 days after reaching stable current density and acetate/methane production. The gas (H_2, CH_4) produced in the MES cathode chamber was measured using a gas chromatograph (GC, SRI Instruments) (Katuri et al., 2014). Acetate concentration in the liquid samples was analyzed using gas chromatograph-mass spectrometry (GC-MS, 7890A, Agilent Technologies) equipped with a flame ionization detector (FID) (Bian et al., 2020b). The temperatures for the injector and FID were set at 150℃ and 250℃, respectively, with a fused silica capillary column (Nukol ™, Supelco Analytical) for compound analysis. The flow rate of the carrier gas (Helium) was 5 mL/min. The liquid sample was mixed with 1% H_3PO_4 (a volume ratio of 9:1) to avoid precipitation before being injected to GC-MS-FID machine. The performance of MES reactors under different operation conditions was evaluated in terms of current density (A/m^2) and methane/acetate production rates ($mmol/m^2/day$). All the parameters here were normalized to the cathode surface area for comparison purposes. The cathodic Coulombic efficiency (CE) was calculated using the equation below.

$$CE = \frac{Q_{chemicals}}{Q_{total}}$$

where $Q_{chemicals}$ is the coulomb required for the production of chemicals (H_2, methane, and acetate) at the cathode in one batch, and Q_{total} is the total coulomb produced by the current in the corresponding batch.

The carbon utilization efficiency (CUE) was also calculated following a similar method described by Bajracharya et al. (Bajracharya et al., 2016). Basically, the conversion ratio for CO_2/acetate is 2:1, while for methane production the conversion ratio for CO_2/CH_4 is 1:1. Besides, in the case of chemolithoautotrophic microbes producing biochemicals from CO_2 and H_2, 5% of the carbon flux utilized above was considered to account for cell synthesis. The carbon utilization efficiency (CUE) was calculated using the equation below.

$$\mathrm{CUE} = \frac{(r_{AC} \times 2 + r_{CH_4}) \times 1.05}{r_{CO_2} \times 60 \times 24/22.4 \,/\, S}$$

where r_{AC} is the acetate production rate (10^{-3} mol/m^2/day) and r_{CH4} is the methane production rate (10^{-3} mol/m^2/day). r_{CO2} is the CO_2 flow rate (L/min), which is converted to L/day by multiplying (60×24) min/day. 22.4 L/mol represents the volume of 1 mol gas at standard temperature and pressure. S is the surface area of the biocathode (0.0035 m^2).

2.5. Microbial community analysis

Genomic DNA was extracted from biofilm and suspension samples using the standard protocol for FastDNA Spin kit for Soil (MP Biomedicals, USA) (Alqahtani et al., 2019). The sequencing libraries for 16S rRNA gene region V4 of Bacteria and Archaea, using forward primer [515FB] GTGYCAGCMGCCGCGGTAA and reverse primer [806RB] GGACTACNVGGGTWTCTAAT, were prepared by a custom protocol based on Illumina. To obtain operational taxonomic unit (OTU) abundances for further statistical analysis, the

bioinformatic processing of the forward and reverse 16S rRNA amplicon reads was conducted following the same procedures reported in a previous study (Alqahtani et al., 2019).

3. Results and discussion

3.1. Selection of better CO_2 delivery method (Phase II)

Before initiation of Phase II, chemolithoautotrophs were enriched for ~150 days with bicarbonate as the sole carbon source. During the enrichment phase (i.e., Phase I), methane production started to be detected after 5 batches of MES operation despite the addition of Na-2-BES to inhibit methanogenesis. To investigate why methanogenesis was not inhibited by Na-2-BES, serum vial experiments were conducted using suspended biomass collected from the MES cathode chamber in Phase I as inoculum. It was found that Na-2-BES (concentration decreased from 15 mM to 9.4 mM) could be reduced to H_2S by sulfate reducing bacteria (SRB) using H_2 or acetate as electron donors, and thus led to the failure of methanogenesis inhibition. The presence of SRB was confirmed later by microbial community analysis (see section 3.3). Based on the above results, magnesium sulfate was replaced by magnesium chloride in DSMZ 879 media to avoid growth of SRB.

After achieving stable acetate and methane production during the enrichment stage, Phase II experiments were initiated to test the effect of CO_2 delivery method on MES performance. From the LSV curves (Fig. 1A) of MES reactors adjusted to the same pH, both direct and indirect CO_2 delivery showed similar onset potential for hydrogen evolution reaction (HER, –756.6 vs. –758.8 mV vs Ag/AgCl). The bulk catholyte pH was slightly lower for direct CO_2 delivery (6.56 ± 0.03) compared to indirect (6.68 ± 0.01). One would expect lower surface pH via continuous longtime buffering with direct CO_2 delivery and

lower onset potential for HER, but due to the limited CO_2 sparging time (20 mins) before LSV tests and short distance between CHT/Ni foam/CNT cathode and plain CHT (~ 2 cm), this difference was not significant. Since the acidic pH usually promotes HER as reported in previous studies (Jourdin et al., 2016a) and hydrogen is believed to serve as the mediator for MES from CO_2 (Bian et al., 2020a; Jourdin et al., 2016b), enhanced HER through lowering the pH by direct CO_2 delivery could be beneficial for biochemical production in MES and thus contributes to better performance of MES. It should be also noted that higher cell density measured by FCM was observed in the suspension during direct delivery ($1.3\pm0.2 \times 10^7$cells/mL) compared to indirect CO_2 delivery ($0.6\pm0.4 \times 10^7$ cells/mL) at a fixed flow rate of 1 ml/min, probably due to the detachment of microbial cells from CHT/Ni foam/CNT biocathode in MES.

The performance of MES was further evaluated in terms of current density, biochemical production and coulombic efficiencies for the two different CO_2 delivery methods. The current density was 1.9 ± 0.1 A/m^2 in direct CO_2 delivery compared to 1.6 ± 0.2 A/m^2 in indirect delivery (Table 1 and Fig. 1B), which were within the range of current densities reported in previous studies using a similar cathode potential of –0.8 V vs Ag/AgCl (e.g. 0.17 A/m^2 with MXene $Ti_3C_2T_x$-coated carbon felt electrode (Tahir et al., 2020) and 3.5 A/m^2 with Si-TiO_2 nanowire photocathode (Liu et al., 2015). It should be noted that a 19% margin between the two current densities was recorded in this study, demonstrating the advantage of direct CO_2 delivery to MES biocathode. However, this difference was not significant ($p = 0.16 > 0.05$ from t-test) as in our previous study (Bian et al., 2018), and it could be attributed to the short distance between CHT/Ni foam/CNT cathode and plain CHT (~ 2 cm) and the way CO_2 gas was indirectly delivered. In our previous study, indirect

CO_2 delivery was conducted by sparging 50 ml 80:20 N_2/CO_2 every 1.5 days through a syringe needle, instead of continuous CO_2 pumping through CHT as is done in the current study. Using a high-speed camera, CO_2 sparging into medium through the syringe needle generated gas bubbles with 7-fold larger size and rising speed in MES medium (data not published) compared to those generated from Ni hollow fibers (Bian et al., 2018). At the same CO_2 flow rate, larger size of gas bubbles generally means lower total interfacial surface area between all gas bubbles and MES medium (Cussler, 2009), which leads to less amount of CO_2 diffused to MES biocathode via indirect CO_2 delivery (Bian et al., 2018).

In terms of biochemical production rates, direct CO_2 delivery through CHT/Ni foam/CNT biocathode achieved 45% higher acetate (29.9 ± 1.42 vs 20.6 ± 2.7 mmol/m^2/day) and 77% higher methane (76.9 ± 6.5 vs 43.5 ± 7.1 mmol/m^2/day) production rates (Table 1), clearly demonstrating the advantages of minimizing the distance of CO_2 (and/or H_2 from the recirculation gasbag) mass transfer to chemolithoautotrophs on biocathode surface. The dual-function CHT/Ni foam/CNT cathode provided a suitable environment to chemolithoautotrophs on the cathode surface where both reducing equivalents (electrons or H_2) and CO_2 were concurrently available to them for product formation. The acetate production rate reported here by direct CO_2 delivery was lower than what has been reported previously (> 1 mol/m^2/day) in MES systems operated at higher cathode potentials (and/or current density) (Jourdin et al., 2015; LaBelle & May, 2017; May et al., 2016), which can generate sufficient hydrogen for bacterial growth and biocatalyzed CO_2 reduction to acetate. However, in another MES study utilizing a mixed culture biocathode and an applied cathode potential (–0.797 V vs Ag/AgCl) similar to our study, the average acetate production was 44-70 mmol/m^2/day for Periods 2 and 3 (450 ml

catholyte) without methane generation (Batlle-Vilanova et al., 2016), which is close to the acetate production rate obtained in this study. Giddings et al. (Giddings et al., 2015) also reported similar acetate production (28-69 mmol/m^2/day with no methane generation) at a cathode potential of ~ –0.85 V vs Ag/AgCl. It should be noted that most of the electrons from the cathode ended up in methane in the current study and acetate production as high as 106.8 mmol/m^2/day could have been achieved if all the electrons ended up in acetate under direct CO_2 delivery. When comparing the methane production, another MES study, however, reported much lower methane production rates (13.7-24.0 mmol/m^2/day) at a cathode potential of –1V vs Ag/AgCl using carbon cloth with limited HER (Ragab et al., 2019). The overall performance of the MES reactors with continuous and direct CO_2 delivery through the biocathodes was superior to indirect CO_2 delivery through the plain CHT (Fig. 1B), and it could be further improved by optimizing the microbial enrichment, cathode potential and minimizing the deposition of insulating compounds such as sulfur or sulfide precipitates by SRB. The cathodic coulombic efficiency for acetate and methane production was 51.5 ± 3.2% with direct CO_2 delivery, which is 16% higher than what is obtained with indirect CO_2 delivery (35.1 ± 4.2%) (Table 1). Furthermore, the CUE for MES with direct CO_2 delivery (0.8%), which was close to what has been reported by Bajracharya et al. (Bajracharya et al., 2016), was 60% higher compared to indirect CO_2 delivery (0.5%). This suggests that microbes on MES cathode could utilize the carbon source more efficiently via direct CO_2 delivery and the carbon source might not be limiting for microbial growth and biochemical production in this study. Instead H_2 (potential reducing equivalent) mass transfer/availability at the biocathode surface, which could be altered by the fluctuation in gaseous CO_2 flow rates through direct CO_2 delivery, was most

likely limiting the CO_2 reduction in MES. Importantly, biochemical production could immediately stabilize within two batches after changing the delivery method, which demonstrates the robustness of the MES system.

3.2. Impact of fluctuations in CO_2 flow rates on MES performance (Phase III)

Based on the results in section 3.1, direct CO_2 delivery through the pores of CHT/Ni foam/CNT biocathode was selected to study the effect of CO_2 flow rate fluctuations. Four different flow rates (0.3, 1, 3 and 10 ml/min) were applied during MES operation and each flow rate lasted for two batches (Table 1). LSV was performed at neutral pH 7 (Fig. 2A) to determine the effect of different flow rates on the onset potential of HER using the same MES biocathode as working electrode. The onset potential of HER slightly decreased (from –758.2 mV to –755.1 mV vs Ag/AgCl) with the increase in flow rates (from 0.3 ml/min to 10 ml/min). In a parallel abiotic LSV test without medium pH control, however, much lower onset potential was observed at 10 ml/min (–391.1 mV vs Ag/AgCl, pH=6.3) compared to 0.3 ml/min (–473.5 mV vs Ag/AgCl, pH=6.8). Even though cathode biofunctionalization has been reported to lower the HER overpotential and facilitate hydrogen production (Marshall et al., 2013; May et al., 2016), the difference in HER onset potential between the abiotic and biotic tests in this study could be probably attributed to the different pH levels, the availability of protons near the cathode surface and the deposition of elemental sulfur (and/or sulfide compounds) on the cathode surface by SRB activities (Bian et al., 2020b). A previous study reported a 2.2 pH gradient from bulk media (6.6) to biocathode surface (8.8) in a microbial electrochemical system (Babauta et al., 2013), which represents more than 100-fold decrease in proton concentration at the cathode

surface and requires higher onset potential for HER according to Nernst equation ($E^{o}_{H_2,pH} = -0.059 \times \mathrm{pH}$, where $E^{o}_{H_2,pH}$ in volts refers to the equilibrium potential for hydrogen evolution as a function of pH at 25°C and 1 atm). It is thus essential to buffer pH at MES biocathode surface via direct CO_2 delivery (Lu et al., 2020). As expected, the bulk pH decreased with increase in CO_2 flow rates (from 6.91 ± 0.04 at 0.3 ml/min to 6.33 ± 0.06 at 10 ml/min) (Fig. 2B). The pH at the interface between Ni foam/CNT cathode and biofilm, which could not be measured with the current MES configuration, is expected to be better buffered than the bulk pH (Lu et al., 2020). As the lower surface pH could potentially leads to more hydrogen production (LaBelle et al., 2014), 10 ml/min CO_2 flow generated 3.9-fold higher hydrogen production (1409.5 ± 75.3 mmol/m^2) than what was obtained at 0.3 ml/min (360.1 ± 8.2 mmol/m^2) in the abiotic test (Table 1). As microbial electrosynthesis of biochemicals from CO_2 was demonstrated to be strongly dependent on medium pH and H_2 production (Jourdin et al., 2016a), slightly lower pH (pH > 5.2) could lead to a significant enhancement of MES performance in terms of biochemical generation and electron consumption. Also, continuous flow of CO_2 in this study avoided the addition of acids to the medium for the formation of slightly acidic environment during MES operation, which is believed to have a technical and economic benefits.

The cell density in suspension was significantly enhanced by the increase in CO_2 flow rate (Fig. 2B), reaching 2.6 ± 0.6 × 10^8 cells/ml at 10 ml/min compared to 7.8 ± 0.4 × 10^7 cells/ml at 3 ml/min (t-test, $p=0.047 < 0.05$). To confirm whether this increment was largely due to cell detachment from CHT/Ni foam/CNT biocathode or growth, we conducted a supplementary experiment using abiotic CHT/Ni foam/CNT cathode and an

initial cell suspension of 6×10^5 cells/ml in MES catholyte measured by FCM. At 10 ml/min, the cell density increased to $3.5 \pm 1.2 \times 10^7$ cells/ml after 12 days of MES operation, suggesting that the increase in cell density and concomitantly increase in H_2 production (Table 1), was mainly due to growth on H_2 and CO_2. Further, this increase in cell density was accompanied by an increase in methane production, supporting the role of suspended biomass in methane generation.

Within each MES batch at different CO_2 flow rates, the electrons were rapidly consumed for HER followed by biotic CO_2 reduction at the beginning, which was reflected by a sharp increase in current density and biochemical production in the first 2-3 days of each batch (Fig. 2C). MES reactors sparged with 10 ml/min CO_2 through CHT/Ni foam/CNT biocathode achieved higher acetate and methane production rates compared to the other three CO_2 flow rates tested (Table 1 and Fig. 2C). No significant difference in methane production rate was noticeable at low flow rates (0.3, 1.0 and 3.0 ml/min), probably due to the lower H_2 supply at these flow rates (Table 1). As methane generation in the cathode chamber is mainly mediated by H_2 produced from HER at the cathode surface (Ragab et al., 2019) and methanogens have been reported to have high H_2 affinity (Molenaar et al., 2017), the MES reactors operated at 10 ml/min with higher hydrogen production (Table 1) resulted in the most noticeable increase in methane production rate where it increased by 196% from 81.2 ± 6.6 mmol/m^2/day at 0.3 mL/min to 240.5 ± 32.2 mmol/m^2/day at 10 mL/min. As mentioned above, suspended biomass density was also higher at CO_2 flow rate of 10 ml/min (Fig. 2B) and they may have also contributed to the increase in the generation of methane in the cathode chamber. The methane production rate at 10 ml/min in this study was 49% higher than an earlier study utilizing Ni hollow fiber cathode for pulse CO_2

delivery and microbial growth (Alqahtani et al., 2018). This suggests that higher biochemical production was achievable by simply regulating the CO_2 flow rates. Acetate production rate exhibited a similar trend like methane generation with increase in CO_2 flow rates, and the increase was not significant for 0.3 ml/min (30.3 ± 8.5 mmol/m^2/day) and 1.0 ml/min (30.6 ± 2.6 mmol/m^2/day) (Table 1 and Fig. 2C). Significant increase in acetate production rate started at 3 ml/min, reaching an average of 45.2 ± 5.3 mmol/m^2/day. This increase could be attributed to the higher supply of H_2 as electron donors for chemolithoautotrophs, which lead to 3 times higher suspended cell density in MES cathode chambers at 3 ml/min compared to lower CO_2 flow rates (Fig. 2B). The biochemical production was comparable to what has been reported in previous studies as mentioned in Section 3.1 above and could be further enhanced by optimizing the enrichment conditions, CO_2 flow rates and inoculum selection.

The increase in acetate and methane production at 10 ml/min was also reflected in the cathodic coulombic efficiencies (CEs) which reached 90.7 ± 11.7% at a CO_2 flow rate of 10 ml/min. The lowest CE obtained was 59.3 ± 2.7% at 3 ml/min, which falls within the normal range of CEs reported in the literature (Bian et al., 2020a). The large difference of CE between high and low flow rates could be possibly attributed to the competitive advantage of SRB over methanogens under H_2-limiting conditions (Robinson & Tiedje, 1984). SRB were more competitive compared to methanogens in serum vial experiments under H_2-limiting conditions (H_2 in headspace), which makes H_2S a sink for a relatively larger portion of electrons at low flow rates. However, CUE exhibited an opposite trends to methane and acetate production (Table 1) at different flow rates. Microbes on the biocathode and in suspension were shown to be more efficient to capture CO_2 at low flow

rates, achieving more than 10 times higher CUE at 0.3 ml/min (2.7%) compared to 10 ml/min. These results suggest that most of the gaseous CO_2 remains unutilized before escaping from the reactor headspace.

The current density also increased with increase in CO_2 flow rates (Fig. 2C and Table 1). At 10 ml/min, the average current density was 2.8 ± 0.2 A/m^2, which represents a 115% increase when compared to the current density obtained at CO_2 flow rate of 0.3 ml/min. In contrast, no sharp improvement in current density was noticed at lower flow rates (from 0.3 to 3 ml/min), which is in good agreement with the results of abiotic H_2, biotic methane and acetate production (Table 1). Since better H_2 bubble detachment and pH buffering could be induced by direct CO_2 delivery, enhanced electron transfer and cathodic HER reaction might be facilitated with faster CO_2 delivery at 10 ml/min (Lu et al., 2020). Therefore, higher current density could be expected with direct CO_2 delivery at 10 ml/min, whereas slower surface reaction kinetics could be induced by low CO_2 flow rates.

Overall, the results above clearly indicate that MES performance in terms of abiotic H_2 evolution, biochemical production and current generation was improved at higher CO_2 flow rates (> 3 ml/min). Also, with the increase in CO_2 flow rates, a larger percentage of electrons ended up in methane generation, which indicates the possible kinetic advantage of methanogens over acetogens under H_2-rich conditions. By simply regulating the CO_2 flow rate, synthesis of specific bioproducts might be feasible in MES system, as illustrated in a previous study (Jourdin et al., 2019).

3.3. Microbial community analysis

High-throughput 16S rRNA gene sequencing was conducted to analyze the biofilm and suspension microbial community during different phases of MES operation. The heatmap

of the top 15 OTUs (relative abundance ≥ 0.1%) detected on the biocathode in Phase I clearly shows the enrichment of chemolithoautotrophs belonging to methanogens (*Methanobacterium*) and acetogens (*Acetobacterium*) from the original anaerobic sludge. The original inoculum was dominated by an unclassified Firmicutes (27.3%, order DTU014) and the genus *Methanobacterium* (12.4%). Species belonging to *Methanobacterium* are hydrogenotrophic methanogens, which can utilize H_2/CO_2 (some members can utilize formate) for methane production and growth under strictly anaerobic conditions (Whitman et al., 2014). The enrichment of *Methanobacterium* (from 12.4% to 51.9 ± 1.4%) and *Acetobacterium* (from 0.4% to 28.6 ± 0.2%), both of which could feed on H_2 and CO_2 (LaBelle et al., 2014; Whitman et al., 2014), could be attributed to the selective pressure of the cathodic hydrogen production in the MES reactors. It is highly possible that H_2-mediated microbial electrosynthesis from CO_2 occurred in this study for the sustainable production of CH_4 and acetate, the mechanism of which has been also reported in previous studies (Alqahtani et al., 2018; LaBelle et al., 2014). In addition to the enrichment of methanogens and acetogens, which accounted for more than 80% of the total reads, sequence reads belonging to OTU_47 and OTU_12 from the family *Desulfovibrionaceae* (phylum Proteobacteria), as well as the genera *Desulfovibrio* and *Desulfomicrobium* (phylum Proteobacteria, family *Desulfovibrionaceae*), represented more than 3% of the total reads, indicating the possible enrichment of SRB in Phase I. This supports the results of serum vial experiments where Na-2-BES might be reduced by SRB to form H_2S.

Methanobacterium and *Acetobacterium* remained the dominant genera on the biocathode (76-84% of the total reads) and suspension (76-84% of the total reads) of Phase II regardless of the CO_2 delivery method (Table 2). However, *Methanobacterium* decreased

from 51.9 ± 1.4% (Phase I) to 43.3 ± 7.7% (Phase II) in the biofilm after direct CO_2 delivery to CHT/Ni foam/CNT biocathode, while *Acetobacterium* increased from 28.6 ± 0.2% (Phase I) to 36.0 ± 4.1% (Phase II). As for indirect CO_2 sparging through plain CHT, *Methanobacterium* accounted for 39.3 ± 5.4% and *Acetobacterium* for 43.0 ± 3.4% of the total reads on the biocathode. The microbial community in suspension exhibited a different characteristic for both CO_2 delivery methods (Table 2) where the relative abundance of *Acetobacterium* with direct CO_2 delivery was significantly higher (48.8 ± 3.4%) than *Methanobacterium* (32.4 ± 0.8%), whereas with indirect CO_2 delivery, the relative abundance of *Methanobacterium* (48.7 ± 0.6%) was higher than *Acetobacterium* (27.6 ± 0.4%). The family *Desulfovibrionaceae* reported in other MES reactors (Rojas et al., 2018) was also found to be more abundant (OTU_47 and OTU_12) in the biofilm compared to suspension. Members of the family *Desulfovibrionaceae* (Rojas et al., 2018), including the genus *Desulfovibrio*, have been reported to catalyze biotic hydrogen production on biocathode, and they may contribute to providing hydrogen to *Methanobacterium* and *Acetobacterium*. Despite significant differences in the rates of methane and acetate production between the two methods (Table 1), the microbial community (Table 2) responsible for methane and acetate generation were predominant (representing 75-85% of the total reads) in both direct and indirect CO_2 delivery. This was also reflected in the principal component analysis (PCA) where the microbial community in cathodic biofilm or suspension were strongly clustered regardless of the delivery method used (Fig. 3A). This lack of difference could be attributed to the fact that amplicon DNA sequencing does not reflect the active members in the community. Future studies using reverse-transcribed

rRNA sequencing should be applied for identifying the active populations in MES (Ragab et al., 2019).

Similar to Phase I and II, *Methanobacterium* and *Acetobacterium* remained dominant members (~ 80% of the total reads) after switching the operation to Phase III (Table 3). Since the biofilm and suspension samples were both dominated by hydrogenotrophic methanogens and acetogens, the microbial electrosynthesis of acetate and methane from CO_2 was mainly dictated by H_2 and CO_2 supply from CHT/Ni foam/CNT biocathode during Phase III. This explains the noticeable increase of methane and acetate formation rates at 10 ml/min compared to the other three flow rates, as much higher H_2 production (1409.5 ± 75.3 mmol/m^2) was observed at10 ml/min in the abiotic test (Table 1). Regardless of the CO_2 flow rates, the relative abundance of genera in MES biofilm responsible for methane (*Methanobacterium*: 37.5-48.3%) and acetate production (*Acetobacterium*: 34.4-41.9%) remained relatively stable. Chloroflexi (2.6-3.5%) and *Desulfovibrionaceae* (1.2-3.3%), reported in other MES biocathodes (Ragab et al., 2019), exhibited similar relative abundance as in Phase II, indicating the relatively high resistance of the cathodic biofilm community to various CO_2 delivery methods and flow rates. The PCA plots further confirmed the resistance of the microbial community to different CO_2 flow rates. The biocathode (as well as suspension) microbial community were strongly clustered in the PCA regardless of CO_2 flow rates (Fig. 3B), while variation between biofilm and suspension was clearly depicted in the PCA plot. As the dominant genera were also *Methanobacterium* (35.6-63.8%) and *Acetobacterium* (10.7-41.4%) among the suspended biomass, the differences between biocathode and suspension community could be mainly associated with the variations in the minor microbial communities as previously

reported (Rojas et al., 2018). The minor microbial community in suspension was composed of family and genera with total relative abundance below 10%, including OTU_6 belonging to the family *Synergistaceae* (phylum Synergistetes), OTU_9 from the family *Spirochaetaceae* (phylum Spirochaetes), genus AUTHM297 (phylum Thermotogae) and genus *Thiomonas* (phylum Proteobacteria) (Table 3). Even though fermenters from the phyla Bacteroidetes, Synergistetes, and Chloroflexi existed as minor communities in both biofilm and suspension, a previous study has revealed that they could produce H_2 and CO_2 from fermentation (Ragab et al., 2019) and possibly grow syntrophically with *Methanobacterium* (Zinder & Koch, 1984). This was partially supported by the serum vial experiments using suspended biomass collected from the cathode chamber where methane was generated using acetate as the electron donor, and no acetoclastic methanogens were detected in both biofilm and suspension samples.

4. Conclusions

This study explores for the first time the robustness of MES system to CO_2 flow fluctuations. Biochemical production was significantly enhanced with higher coulombic efficiency (51.5%) via direct CO_2 delivery to microbes. Minor increment in biochemical production was initiated at low CO_2 flow rates, while higher methane (240.0 ± 32.2 mmol/m^2/day) and acetate (47.0 ± 18.4 mmol/m^2/day) production was observed at 10 ml/min. Microbial community in biofilm and suspension, dominated by *Methanobacterium* and *Acetobacterium* for possible H_2-mediated methane and acetate production, exhibited high resistance to changes in CO_2 delivery methods and flow rates, bringing MES system closer to real-field implementation.

Acknowledgements

This work was supported by Competitive Research Grant (URF/1/2985-01-01) from King Abdullah University of Science and Technology (KAUST).

Supplementary material

E-supplementary data of this work can be found in online version of the paper.

References

1. Alqahtani, M. F., Bajracharya, S., Katuri, K. P., Ali, M., Ragab, A., Michoud, G., Daffonchio, D., Saikaly, P. E. 2019. Enrichment of Marinobacter sp. and Halophilic Homoacetogens at the Biocathode of Microbial Electrosynthesis System Inoculated With Red Sea Brine Pool. *Front. Microbiol.*, **10**, 2563.

2. Alqahtani, M. F., Katuri, K. P., Bajracharya, S., Yu, Y. L., Lai, Z. P., Saikaly, P. E. 2018. Porous Hollow Fiber Nickel Electrodes for Effective Supply and Reduction of Carbon Dioxide to Methane through Microbial Electrosynthesis. *Adv. Funct. Mater*, **28**(43), 1804860.

3. Anantharaman, R., Roussanaly, S., Westman, S. F., Husebye, J. 2013. Selection of optimal CO2 capture plant capacity for better investment decisions. *Ghgt-11*, **37**, 7039-7045.

4. Aryal, N., Halder, A., Zhang, M., Whelan, P. R., Tremblay, P. L., Chi, Q., Zhang, T. 2017a. Freestanding and flexible graphene papers as bioelectrochemical cathode for selective and efficient CO2 conversion. *Sci. Rep.*, **7**(1), 9107.

5. Aryal, N., Tremblay, P. L., Lizak, D. M., Zhang, T. 2017b. Performance of different Sporomusa species for the microbial electrosynthesis of acetate from carbon dioxide. *Bioresour. Technol.*, **233**, 184-190.

6. Babauta, J. T., Nguyen, H. D., Istanbullu, O., Beyenal, H. 2013. Microscale gradients of oxygen, hydrogen peroxide, and pH in freshwater cathodic biofilms. *ChemSusChem*, **6**(7), 1252-1261.

7. Bajracharya, S., Vanbroekhoven, K., Buisman, C. J., Pant, D., Strik, D. P. 2016. Application of gas diffusion biocathode in microbial electrosynthesis from carbon dioxide. *Environ. Sci. Pollut. Res. Int.*, **23**(22), 22292-22308.

8. Batlle-Vilanova, P., Puig, S., Gonzalez-Olmos, R., Balaguer, M. D., Colprim, J. 2016. Continuous acetate production through microbial electrosynthesis from CO2 with microbial mixed culture. *Journal of Chemical Technology and Biotechnology*, **91**(4), 921-927.

9. Bian, B., Alqahtani, M. F., Katuri, K. P., Liu, D. F., Bajracharya, S., Lai, Z. P., Rabaey, K., Saikaly, P. E. 2018. Porous nickel hollow fiber cathodes coated with CNTs for efficient microbial electrosynthesis of acetate from CO2 using Sporomusa ovata. *J. Mater. Chem. A*, **6**(35), 17201-17211.

10. Bian, B., Bajracharya, S., Xu, J., Pant, D., Saikaly, P. E. 2020a. Microbial electrosynthesis from CO2: Challenges, opportunities and perspectives in the context of circular bioeconomy. *Bioresour. Technol.*, **302**, 122863.

11. Bian, B., Shi, L., Katuri, K. P., Xu, J., Wang, P., Saikaly, P. E. 2020b. Efficient solar-to-acetate conversion from CO2 through microbial electrosynthesis coupled with stable photoanode. *Appl. Energy*, **278**, 115684.

12. Cussler, E. L. 2009. Fundamentals of Mass Transfer. 3 ed. in: *Diffusion: Mass Transfer in Fluid Systems*, (Ed.) E.L. Cussler, Cambridge University Press. Cambridge, pp. 237-273.

13. Giddings, C. G., Nevin, K. P., Woodward, T., Lovley, D. R., Butler, C. S. 2015. Simplifying microbial electrosynthesis reactor design. *Front. Microbiol.*, **6**, 468.

14. Jourdin, L., Freguia, S., Flexer, V., Keller, J. 2016a. Bringing High-Rate, CO2-Based Microbial Electrosynthesis Closer to Practical Implementation through Improved Electrode Design and Operating Conditions. *Environ. Sci. Technol.*, **50**(4), 1982-1989.

15. Jourdin, L., Grieger, T., Monetti, J., Flexer, V., Freguia, S., Lu, Y., Chen, J., Romano, M., Wallace, G. G., Keller, J. 2015. High Acetic Acid Production Rate Obtained by Microbial Electrosynthesis from Carbon Dioxide. *Environ. Sci. Technol.*, **49**(22), 13566-13574.

16. Jourdin, L., Lu, Y., Flexer, V., Keller, J., Freguia, S. 2016b. Biologically Induced Hydrogen Production Drives High Rate/High Efficiency Microbial Electrosynthesis of Acetate from Carbon Dioxide. *Chemelectrochem*, **3**(4), 581-591.

17. Jourdin, L., Winkelhorst, M., Rawls, B., Buisman, C. J. N., Strik, D. P. B. T. B. 2019. Enhanced selectivity to butyrate and caproate above acetate in continuous bioelectrochemical chain elongation from CO2: Steering with CO2 loading rate and hydraulic retention time. *Bioresour Technol Rep*, **7**, 100284.

18. Jung, S., Lee, J., Park, Y. K., Kwon, E. E. 2020. Bioelectrochemical systems for a circular bioeconomy. *Bioresour. Technol.*, **300**, 122748.

19. Katuri, K. P., Kalathil, S., Ragab, A., Bian, B., Alqahtani, M. F., Pant, D., Saikaly, P. E. 2018. Dual-Function Electrocatalytic and Macroporous Hollow-Fiber Cathode for Converting Waste Streams to Valuable Resources Using Microbial Electrochemical Systems. *Adv Mater*, **30**(26), 1707072.

20. Katuri, K. P., Werner, C. M., Jimenez-Sandoval, R. J., Chen, W., Jeon, S., Logan, B. E., Lai, Z., Amy, G. L., Saikaly, P. E. 2014. A novel anaerobic electrochemical membrane bioreactor (AnEMBR) with conductive hollow-fiber membrane for treatment of low-organic strength solutions. *Environ. Sci. Technol.*, **48**(21), 12833-41.

21. LaBelle, E. V., Marshall, C. W., Gilbert, J. A., May, H. D. 2014. Influence of acidic pH on hydrogen and acetate production by an electrosynthetic microbiome. *PLoS One*, **9**(10), 109935.

22. LaBelle, E. V., May, H. D. 2017. Energy Efficiency and Productivity Enhancement of Microbial Electrosynthesis of Acetate. *Front. Microbiol.*, **8**, 756.

23. Liu, C., Gallagher, J. J., Sakimoto, K. K., Nichols, E. M., Chang, C. J., Chang, M. C., Yang, P. 2015. Nanowire-bacteria hybrids for unassisted solar carbon dioxide fixation to value-added chemicals. *Nano Lett*, **15**(5), 3634-9.

24. Lu, X., Zhu, C., Wu, Z., Xuan, J., Francisco, J. S., Wang, H. 2020. In Situ Observation of the pH Gradient near the Gas Diffusion Electrode of CO2 Reduction in Alkaline Electrolyte. *J. Am. Chem. Soc.*, **142**(36), 15438-15444.

25. Marshall, C. W., Ross, D. E., Fichot, E. B., Norman, R. S., May, H. D. 2013. Long-term operation of microbial electrosynthesis systems improves acetate production by autotrophic microbiomes. *Environ. Sci. Technol.*, **47**(11), 6023-9.

26. May, H. D., Evans, P. J., LaBelle, E. V. 2016. The bioelectrosynthesis of acetate. *Curr. Opin. Biotechnol.*, **42**, 225-233.

27. Molenaar, S. D., Saha, P., Mol, A. R., Sleutels, T. H., Ter Heijne, A., Buisman, C. J. 2017. Competition between Methanogens and Acetogens in Biocathodes: A Comparison between Potentiostatic and Galvanostatic Control. *Int. J. Mol. Sci.*, **18**(1), 204.

28. Ojeda, F., Bakonyi, P., Buitron, G. 2017. Improvement of methane content in a hydrogenotrophic anaerobic digester via the proper operation of membrane module integrated into an external-loop. *Bioresour. Technol.*, **245**, 1294-1298.

29. Peces, M., Astals, S., Mata-Alvarez, J. 2013. Response of a sewage sludge mesophilic anaerobic digester to short and long-term thermophilic temperature fluctuations. *Chem. Eng. J,* **233**, 109-116.

30. Prest, E. I., El-Chakhtoura, J., Hammes, F., Saikaly, P. E., van Loosdrecht, M. C., Vrouwenvelder, J. S. 2014. Combining flow cytometry and 16S rRNA gene pyrosequencing: a promising approach for drinking water monitoring and characterization. *Water Res,* **63**, 179-189.

31. Ragab, A., Katuri, K. P., Ali, M., Saikaly, P. E. 2019. Evidence of Spatial Homogeneity in an Electromethanogenic Cathodic Microbial Community. *Front. Microbiol.*, **10**, 1747.

32. Robinson, J. A., Tiedje, J. M. 1984. Competition between sulfate-reducing and methanogenic bacteria for H2 under resting and growing conditions. *Arch. Microbiol.*, **137**(1), 26-32.

33. Rojas, M. D. A., Mateos, R., Sotres, A., Zaiat, M., Gonzalez, E. R., Escapa, A., De Wever, H., Pant, D. 2018. Microbial electrosynthesis (MES) from CO2 is resilient to fluctuations in renewable energy supply. *Energy Convers. Manag*, **177**, 272-279.

34. Tahir, K., Miran, W., Jang, J., Shahzad, A., Moztahida, M., Kim, B., Lee, D. S. 2020. A novel MXene-coated biocathode for enhanced microbial electrosynthesis performance. *Chem. Eng. J,* **381**

35. Whitman, W. B., Bowen, T. L., Boone, D. R. 2014. *The Methanogenic Bacteria*.Springer, Berlin, Heidelberg.

36. Zinder, S. H., Koch, M. 1984. Non-Aceticlastic Methanogenesis from Acetate - Acetate Oxidation by a Thermophilic Syntrophic Coculture. *Arch. Microbiol.*, **138**(3), 263-272.

Figure and Table Captions

Scheme 1 Direct CO_2 delivery to microbes through pores of CHT/Ni foam/CNT biocathode (left) and indirect CO_2 sparging through electrically insulated ceramic hollow tube (CHT) (right), created using BioRender.

Figure 1 (A) Linear sweep voltammetry (LSV) for different delivery methods (Phase II) at a scan rate of 5 mV/s using the same MES biocathode as working electrode and the same pH. The scan range of LSV is from open circuit potential to –1V vs Ag/AgCl. (B) MES performance in terms of current density, methane and acetate production measured under different delivery methods in Phase II. Results from duplicate MES reactors are presented as mean ± SD.

Figure 2 (A) Linear sweep voltammetry for different flow rates (Phase III) at a scan rate of 5 mV/s using the same MES biocathode as working electrode. The scan range was from open circuit potential to –1V vs Ag/AgCl. (B) Catholyte pH and suspended cell density measured using flow cytometry for different flow rates at the end of the second batch in Phase III. (C) MES performance in terms of current density, methane and acetate production measured at different flow rates. Results from duplicate MES reactors are presented as mean ± SD.

Figure 3 Principal component analysis conducted based on operational taxonomic units of cathodic biofilms and suspension in (A) Phase II and (B) Phase III. Red dots: suspension in MES reactor 1 (R1) or 2 (R2) with direct (DiS)/indirect (InS) CO_2 delivery or at a flow rate (ml/min) of 0.3 (FR03S), 1 (FR1S), 3 (FR3S) and 10 (FR10S). Black dots: biofilm samples from biocathode in reactor 1 (R1) or 2 (R2) with direct (DiC)/indirect (InC) CO_2 delivery or at a flow rate (ml/min) of 0.3 (FR03C), 1 (FR1C), 3 (FR3C) and 10 (FR10C).

Table 1 MES performance during the different phases of long-term reactor operation

Table 2 Heatmap of the 15 most abundant phylotypes across all samples in phase II.

Table 3 Heatmap of the 15 most abundant phylotypes across all samples at different flow rates.

Table 1 MES performance during the different phases of long-term reactor operation

Phases[#]	I	II-a	II-b	III-a	III-b	III-c	III-d
Delivery method	NA[$]	Direct	Indirect	Direct			
Days	~150	25	25	25	25	25	25
Flow rate (ml/min)	0	1	1	0.3	1	3	10
Abiotic H_2 production in 24 hours ($mmol/m^2$)	48.1 ± 11.5	-[*]	-[*]	360.1 ± 8.2	530.6 ± 3.4	689.1 ± 174.5	1409.5 ± 75.3
Current density (A/m^2) [£]	1.1 ± 0.3	1.9 ± 0.1	1.6 ± 0.2	1.3 ± 0.2	1.6 ± 0.1	1.9 ± 0.1	2.8 ± 0.2
Acetate production ($mmol/m^2/day$) [£]	15.3 ± 3.2	29.9 ± 1.2	20.6 ± 2.7	30.3 ± 8.5	30.6 ± 2.6	45.2 ± 5.3	47.0 ± 18.4
Methane production ($mmol/m^2/day$) [£]	38.1 ± 9.0	76.9 ± 6.5	43.5 ± 7.1	81.2 ± 6.6	76.4 ± 9.7	79.2 ± 1.9	240.0 ± 32.2
Carbon utilization efficiency (%)	-[*]	0.8	0.5	2.7	0.8	0.3	0.2
Cathodic CE (%) [£]	41.2 ± 7.4	51.5 ± 3.2	35.1 ± 4.2	74.3 ± 7.2	61.3 ± 5.8	59.3 ± 2.7	90.7 ± 11.7

[#] Phase I (~150 days): enrichment phase. Phase II (50 days): test the effect of direct vs. indirect CO_2 delivery. Phase III (100 days): test the effect of different CO_2 flow rates (0.3, 1, 3 and 10 ml/min); [$] bicarbonate was used as sole carbon source without CO_2 gas sparging; [*] Not measured; [£] Each operation condition in Phase II and Phase III was maintained for two batches. Data from the one of the batches (with better MES performance) is presented here. All values in the table are averages of duplicate reactors.

Table 2 Heatmap of the 15 most abundant phylotypes across all samples in phase II.

	MES Biocathode Biofilm				MES Suspended Biomass			
Taxa Level [#]	Direct CO_2 delivery		Indirect CO_2 delivery		Direct CO_2 delivery		Indirect CO_2 delivery	
Euryarchaeota; g_Methanobacterium	35.6	50.9	33.9	44.7	33.2	31.6	49.2	48.1
Firmicutes; g_Acetobacterium	40.1	31.9	46.3	39.6	45.4	52.2	27.2	27.9
Proteobacteria; f_Desulfovibrionaceae_OTU_47	5.8	1.5	4.1	1	1	0.2	0.5	0.2
Chloroflexi; o_SBR1031	3.2	3.3	2.4	3.3	0.1	0.1	0.2	0.2
WPS-2; g_Burkholderiales-bacterium-Beta_02	0.6	0.3	1.1	0.4	1.1	1.8	1.4	2.6
Spirochaetes; f_Spirochaetaceae_OTU_9	0.1	0.1	0.2	0.2	1.2	1.4	3	2.7
Bacteroidetes; g_Petrimonas	0.4	0.7	0.6	0.9	2.6	1.3	0.7	1
Proteobacteria; g_Azospira	0	0	0	0	1.5	2.4	1.2	3
Proteobacteria; g_Thiomonas	0.1	0.2	0	0.1	1.1	1	3.1	2.4
Proteobacteria; g_Desulfovibrio	1	1	0.3	0.7	1.3	0.8	1	1.9
Synergistetes; g_Aminiphilus	0.5	0.5	0.5	0.5	0.4	0.7	2.1	1.5
Thermotogae; g_AUTHM297	0	0	0	0	0.4	1.5	1	1.6
Proteobacteria; f_Desulfovibrionaceae_OTU_12	1	1.1	0.7	0.9	0.4	0.1	0.2	0.1
Synergistetes; f_Synergistaceae_OTU_6	0	0	0	0	0.4	0.3	2	1.4
Proteobacteria; g_Desulfomicrobium	1.7	0.9	0.7	0.3	0	0	0	0
	Biocathode R1	Biocathode R2	Biocathode R1	Biocathode R2	Suspension R1	Suspension R2	Suspension R1	Suspension R2

[#] The taxa level shown on the left-hand side represents the phyla and the lowest classification level possible (o: order, f: family, or g: genus).

Table 3 Heatmap of the 15 most abundant phylotypes across all samples at different flow rates.

	Biocathode Biofilm								Suspended Biomass							
Taxa Level [#]	0.3		1		3		10		0.3		1		3		10	
Euryarchaeota; g_Methanobacterium	39.5	49.2	39.7	42.8	34.8	40.1	45.9	50.7	55.4	63.8	36.8	37.6	42.2	41	35.6	41.6
Firmicutes; g_Acetobacterium	42.6	35.1	40.6	36.6	44.8	39	36.3	32.4	12.5	10.7	41.1	41.4	23.3	22.2	37.6	29.9
Synergistetes; f_Synergistaceae_OTU_6	0.1	0	0.1	0.1	0.1	0.1	0.1	0	5.2	4.4	2.3	2.2	7.9	8	7.3	5.6
Proteobacteria; g_Thiomonas	0.1	0.1	0.2	0.3	0.1	0	0	0.1	2.9	1.5	4.5	3.9	4.7	5.4	2.8	3.2
Chloroflexi; o_SBR1031	2.6	3.5	3.4	3	2.7	3.3	2.6	3.4	0.3	0.2	0.1	0.1	0.5	0.4	0.4	0.4
Spirochaetes; f_Spirochaetaceae_OTU_9	0.2	0.2	0.2	0.3	0.2	0.2	0.3	0.2	2.1	2.3	2.3	1.9	3.6	3.4	2.1	2.4
Proteobacteria; g_Desulfovibrio	0.3	0.6	1	1.5	0.5	0.4	0.7	1	2.4	3.1	1.1	1.7	2	2.8	0.7	1.9
Synergistetes; g_Aminiphilus	0.7	0.5	0.7	0.5	0.9	0.8	1.1	0.5	2.1	1.7	1	0.4	1.6	1.8	1.8	1.4
Epsilonbacteraeota; o_Campylobacterales	0	0	0	0	0	0	0	0	6	1.1	0.7	0.6	1.1	2.3	1.5	2.5
Bacteroidetes; g_Petrimonas	0.8	0.9	0.8	0.9	0.8	0.7	0.9	1	0.7	0.7	1.2	1.4	1	0.8	0.7	0.9
Bacteroidetes; g_Blvii28−wastewater−sludge−group	0.9	0.3	1.6	1.2	1.8	1.6	1.4	0.4	0.2	0.1	0.4	0.4	0.6	0.7	1.1	0.4
Thermotogae; g_AUTHM297	0	0	0	0	0	0	0	0	2	0.7	0.7	0.6	2.8	2.4	1.2	0.5
Bacteroidetes; g_Lentimicrobium	0.8	0.3	1.2	1.1	2.3	2.5	1.2	0.2	0	0.1	0.1	0.1	0.1	0.3	0.3	0.2
Thermotogae; g_Mesotoga	0.9	0.5	1.1	1.3	0.9	0.8	1.2	0.5	0.4	0.4	0.1	0.1	0.6	0.5	0.8	0.6
Proteobacteria; f_Desulfovibrionaceae_OTU_47	1.6	0.7	1.3	1.8	1.2	0.8	0.5	0.6	0.1	0.1	0.1	0.3	0	0.1	0	0.1
	R1 Biocathode	R2 Biocathode	R1 Biocathode	R2 Biocathode	R1 Biocathode	R2 Biocathode	R1 Biocathode	R2 Biocathode	R1 Suspension	R2 Suspension	R1 Suspension	R2 Suspension	R1 Suspension	R2 Suspension	R1 Suspension	R2 Suspension

[#] The taxa level shown on the left-hand side represents the phyla and the lowest classification level possible (o: order, f: family, or g: genus).

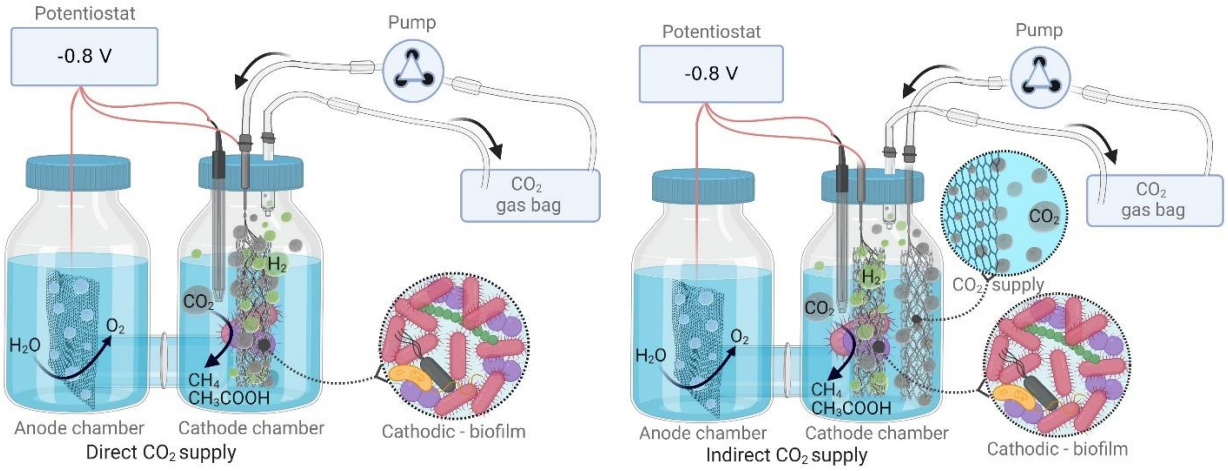

Scheme 1 Direct CO_2 delivery to microbes through pores of CHT/Ni foam/CNT biocathode (left) and indirect CO_2 sparging through electrically insulated ceramic hollow tube (CHT) (right), created using BioRender.

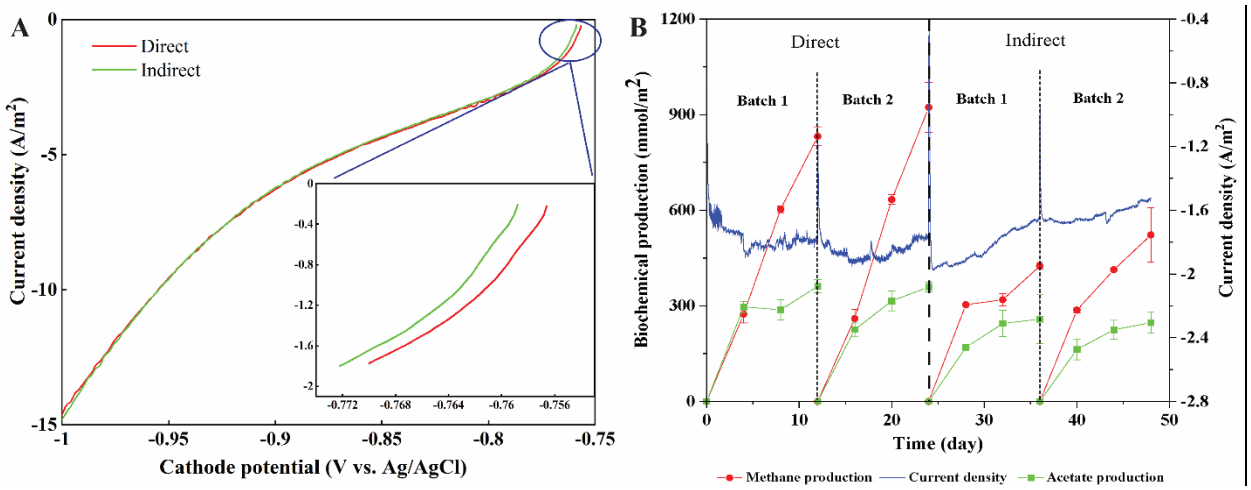

Figure 2 (A) Linear sweep voltammetry (LSV) for different delivery methods (Phase II) at a scan rate of 5 mV/s using the same MES biocathode as working electrode and the same pH. The scan range of LSV is from open circuit potential to –1V vs Ag/AgCl. (B) MES performance in terms of current density, methane and acetate production measured under different delivery methods in Phase II. Results from duplicate MES reactors are presented as mean ± SD.

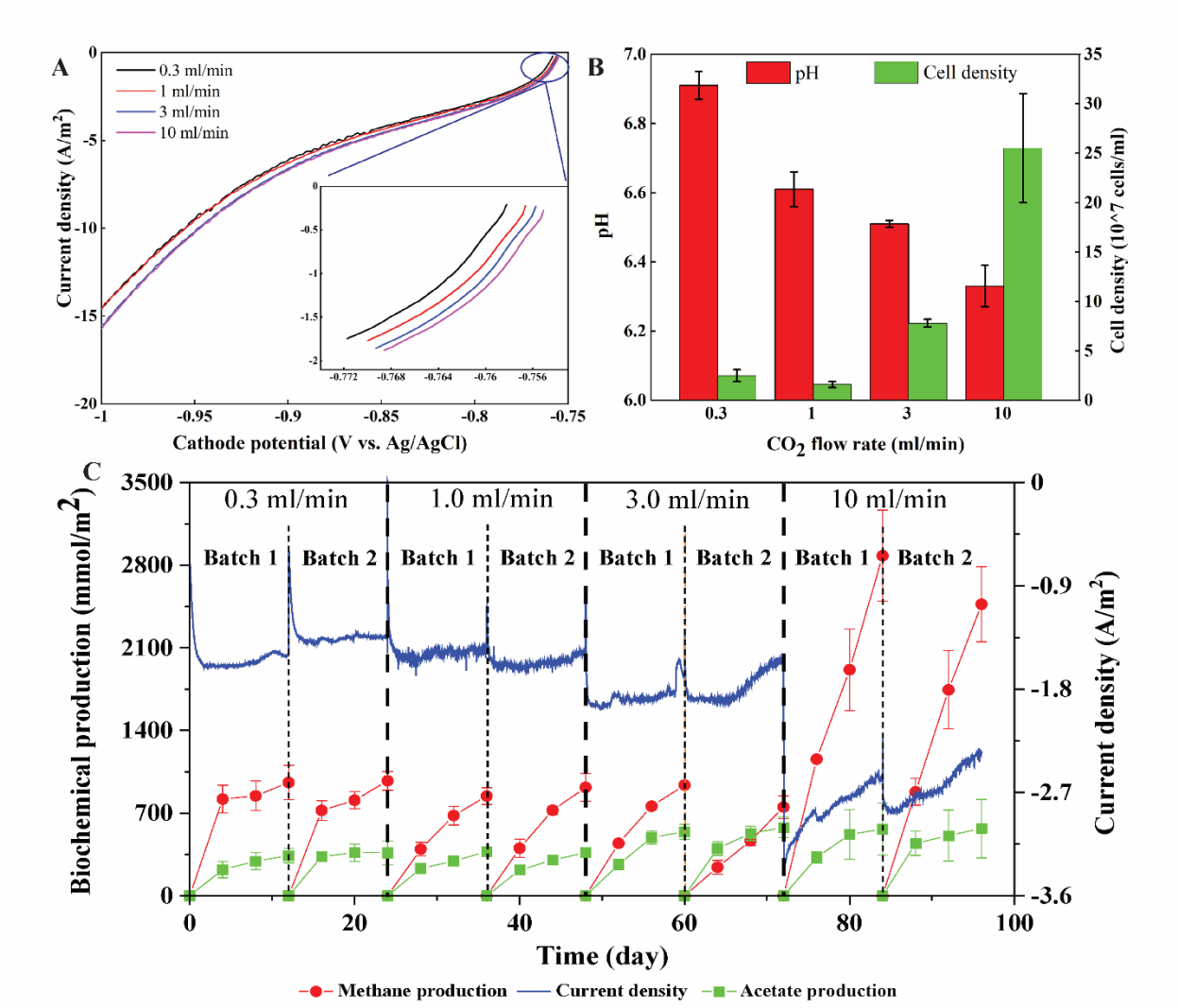

Figure 2 (A) Linear sweep voltammetry for different flow rates (Phase III) at a scan rate of 5 mV/s using the same MES biocathode as working electrode. The scan range was from open circuit potential to –1V vs Ag/AgCl. (B) Catholyte pH and suspended cell density measured using flow cytometry for the four different flow rates at the end of the second batch in Phase III. (C) MES performance in terms of current density, methane and acetate production measured under different flow rates. Results from duplicate MES reactors are presented as mean ± SD.

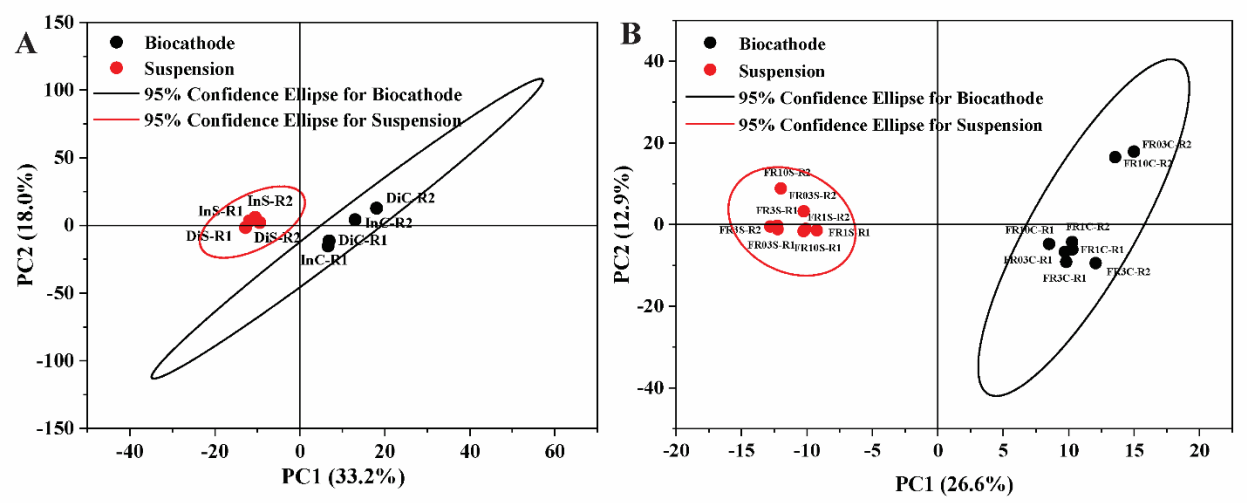

Figure 3 Principal component analysis conducted based on operational taxonomic units of cathodic biofilms and suspension in (A) Phase II and (B) Phase III. Red dots: suspension in MES reactor 1 (R1) or 2 (R2) with direct (DiS)/indirect (InS) CO_2 delivery or at a flow rate (ml/min) of 0.3 (FR03S), 1 (FR1S), 3 (FR3S) and 10 (FR10S). Black dots: biofilm samples from biocathode in reactor 1 (R1) or 2 (R2) with direct (DiC)/indirect (InC) CO_2 delivery or at a flow rate (ml/min) of 0.3 (FR03C), 1 (FR1C), 3 (FR3C) and 10 (FR10C).